



## ORIGINAL ARTICLE

# Suppression of methane explosion in pipeline network by carbon dioxide-driven calcified montmorillonite powder



Wang Fengxiao <sup>a,b,1</sup>, Jia Jinzhang <sup>a,b,1,\*</sup>, Tian Xiuyuan <sup>a,b</sup>

<sup>a</sup> College of Safety Science and Engineering, Liaoning Technical University, Fuxin, Liaoning 123000, China

<sup>b</sup> Key Laboratory of Mine Thermal Power Disaster and Prevention of Ministry of Education, Liaoning Technical University, Huludao, Liaoning 125100, China

Received 12 May 2022; accepted 12 July 2022

Available online 16 July 2022

## KEYWORDS

Suppression of methane explosion in pipe network;  
Carbon dioxide;  
Calcified montmorillonite powder;  
Particle size of powder;  
Explosion suppression mechanism

**Abstract** To minimize the damage and loss caused by methane explosions, and improve the safety of methane extraction, transportation, and utilization, we conducted a study on the explosion suppression performance of carbon dioxide-driven calcified montmorillonite powders with different particle sizes in a custom-designed experimental platform. The explosion suppression performance under different working conditions was evaluated according to the peak explosion overpressure, explosion power index, and the time required to reach the two outlets of the pipe network, and the explosion suppression mechanism was analyzed and discussed. The results indicated that calcified montmorillonite powder showed excellent explosion suppression performance. When the particle size of the powder was 21–32  $\mu\text{m}$  and successively increased to 61–72  $\mu\text{m}$ , both the explosion overpressure and explosion flame were effectively suppressed. In addition, when the particle size of the powder continued to increase to 81–92  $\mu\text{m}$ , it had little enhanced suppression effect on the methane explosion. Therefore, considering the cost of use in practical applications, the calcified montmorillonite powder with a particle size of 61–72  $\mu\text{m}$  was the optimal detonation inhibitor. Based on calcified montmorillonite, compound explosion suppression using carbon dioxide could serve as a theoretical reference and support for further improving the safety of methane extraction, transportation, and utilization.

© 2022 The Author(s). Published by Elsevier B.V. on behalf of King Saud University. This is an open access article under the CC BY-NC-ND license (<http://creativecommons.org/licenses/by-nc-nd/4.0/>).

<sup>1</sup> Wang Fengxiao and Jia Jinzhang contributed equally to this work.

\* Corresponding author.

E-mail address: [jiajinzhang@Intu.edu.cn](mailto:jiajinzhang@Intu.edu.cn) (J. Jinzhang).

Peer review under responsibility of King Saud University.



## 1. Introduction

In recent years, the exploitation of methane gas has increased with continuous improvements in the methane utilization rate. As a flammable and explosive substance, methane can easily explode accidentally. Once a methane explosion occurs, it can pose a major threat to human life and cause immeasurable losses. Therefore, studying efficient methane explosion suppression methods and technologies to reduce the harm of methane explosions is of great practical significance for disaster prevention and reduction (Zhou et al., 2021; Wang et al., 2021; Jia et al., 2022). Inhibitors commonly used in existing studies include fine water mist, inert gas, compound sol, porous media materials, and solid powders (Kundu et al., 2016; Cheng et al., 2012).

Fine water mist suppresses explosions mainly through two reaction mechanisms, namely, endothermic cooling and water vapor dilution. The process of continuous water vapor evaporation under high temperatures will have an obvious dilution effect on combustible gases, while at the same time, fine water mist can effectively reduce the thermal radiation effect of the flame wave (Cao et al., 2016). When fine water mist acts on a flame, it will also affect the flame structure, achieving the purpose of explosion suppression by interfering with the normal formation process of the flame wave (Jing et al., 2021). The explosion suppression effect of fine water mist will be mainly affected by factors such as the water mist amount, density, and particle size. An insufficient amount of water mist will increase the explosion intensity, and when the amount of water mist increases to a certain extent, the increase in the degree of the explosion suppression effect will show a decreasing trend (Wen et al., 2019).

When a combustible gas explodes, the inert gas will reduce the volume fraction of the combustible gas in the system, exhibiting a dilution effect on the combustible gas and effectively affecting the mass transfer process of the combustible gas explosion reaction (Cui et al., 2018; Zhang et al., 2020). In addition, the inert gas, like carbon dioxide, nitrogen, helium, will have a certain endothermic effect in the reaction system, suppressing the mass transfer process and heat transfer degree of the explosion flame wave. In addition, the inert gas in the system will effectively reduce the combustion rate of laminar flame, and the combustion stability of the flame will be enhanced to a certain extent, avoiding the explosion overpressure and flame deflagration caused by flame instability in the middle and later stages of the explosion (Wang et al., 2019). Under the endothermic effect of the inert gas, the flame wave will be continuously stretched during the propagation process, and its structure will present an asymmetrical shape, causing the shock wave compression of the unburned gas to continuously decrease, delaying heat transfer between the burned and the unburned areas. In addition, the mass transfer can destroy the acceleration mechanism of the interactions between the shock and flame waves, effectively suppressing the propagation of the flame wave (Yang et al., 2019).

At present, cold aerosols for suppressing methane explosions have mainly consisted of compound aerosol powders. Cold aerosols offer compressibility, fluidity, and dispersibility, with superior fire extinguishing efficiency compared to other gases, as well as the advantages of being convenient for storage, realizing large flow and long-distance spraying (Guo et al., 2019; Wang et al., 2021). Aerosols can increase the flow distance of heat and the exchange area of high-temperature gases, thereby improving the heat storage and cooling capacity (Wang et al., 2021).

The complex pores of porous media materials will increase the collision probability between free radicals and pore walls, reducing the number of free radicals that can participate in the reaction and suppressing the formation and propagation of a flame (Wang et al., 2020). Thus, a portion of the shock wave generated by the explosion will be absorbed by the porous media materials and will be reflected and scattered many times in the tiny holes, resulting in energy loss. As a result, the overpressure of the explosion shock wave will continue to attenuate, achieving the effect of explosion suppression (Yu et al., 2022).

The powder explosion suppression materials have been widely studied due to their advantages of non-polluting, convenient storage and transportation (Dong et al., 2012; Li et al., 2020; Jiang et al., 2020; Song and Zhang, 2018). Existing research has shown that powders can be used as an effective explosion suppression measure, and many types of powders have been used as explosion suppression agents. For example, Sun et al. (Sun et al., 2019) introduced a novel multi-component powder methane explosion inhibitor, which was prepared by mixing ammonium polyphosphate and aluminum hydroxide with porous kaolinite. The methane explosion suppression experiment was carried out using a 20 L spherical explosion cavity, showing better explosion suppression performance. Yang et al. (Yang et al., 2021) studied the suppression effect of modified attapulgite powder on methane explosions and analyzed and discussed its explosion suppression mechanism. Luo et al. (Luo et al., 2019) studied sodium bicarbonate powder for its ability to suppress methane/hydrogen/air mixture gas explosions and found that the optimum explosion suppression concentration of the sodium bicarbonate powder to suppress methane/air was 200 g/m<sup>3</sup>. Wang et al. (Wang et al., 2019) studied the synergistic suppression performance of carbon dioxide and sodium bicarbonate powder on methane explosion in a 20L spherical explosion experimental system, and Jiang et al. (Jiang et al., 2016) studied the synergistic suppression performance of nitrogen and ammonium hydrogen phosphate powder on methane explosion in a long straight pipeline. The research results all prove that the detonation suppression performance is better when the inert gas and powder are synergistically suppressed.

Montmorillonite is an abundant magnesium-aluminosilicate mineral with a large specific surface area and layered pore structure. This layered structure offers good heat absorption performance when used to modify inhibitors. According to the main cation species between the different pore layers, montmorillonite can be divided into sodium montmorillonite, calcified montmorillonite, and other component variants. Existing studies have demonstrated that montmorillonite powder offers excellent suppression characteristics for methane explosions (Yu et al., 2020; Wang et al., 2021).

For the safety of methane transportation in the current actual pipeline network, it is pretty significant to explore an efficient cooperative explosion suppression method to effectively ensure the safety of methane transportation under actual conditions. In this work, carbon dioxide-driven calcified montmorillonite powder was used in experiments to synergistically suppress methane explosions in an experimental pipe network, and the suppression mechanism was discussed. The conclusions from this study may serve as a theoretical reference for reducing methane explosion accidents and improving the utilization rate of methane and transportation safety.

## 2. Experimental setup and preparation

### 2.1. Experimental system

As shown in Fig. 1, the size of the experimental pipe network was 8100 mm × 5500 mm, the diameter of the pipe was 500 mm. The experimental system was composed of an experimental pipe network, an inert gas generation system, a dynamic data acquisition system, and an ignition system. A data acquisition system (model TST6300) was used to collect the data in real-time, which consisted of a high-speed dynamic data acquisition device (model CR6300), high precision pressure sensors (model CYG1721), and photosensitive flame sensors (model CKG100). The response time of the pressure sensor and flame sensor was 1 ms, the accuracy of the data acquisition device was 0.2% FS (full scale). The ignition system mainly included a DX-GDH high-energy igniter, high-energy sparkplugs, high-voltage-resistant and high-temperature-resistant cables, power supply cables, and exter-

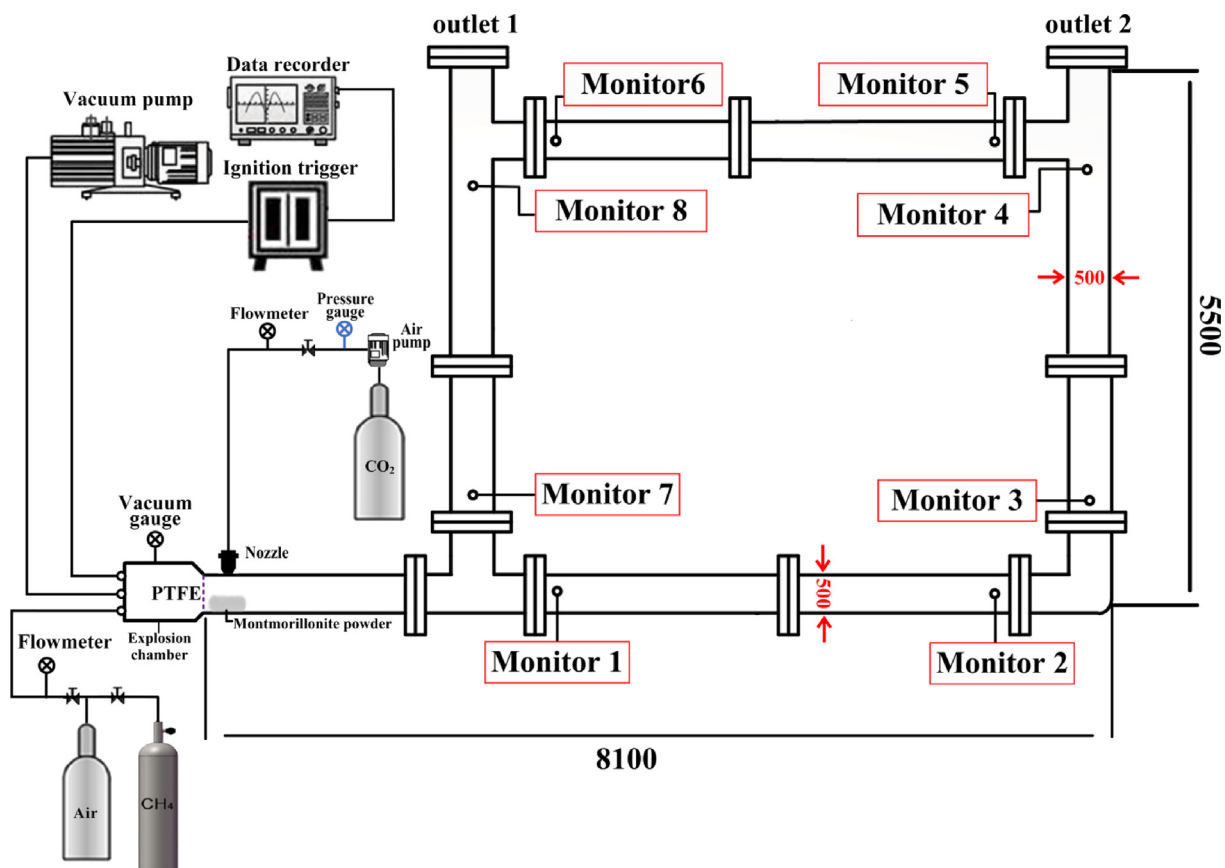


Fig. 1 Experimental system.

nal trigger devices. The ignition control box was connected with an external trigger wire. In addition, the sparkplugs were placed at the front end of the explosion chamber, where the ignition voltage was about 2200 V, and the one-time energy storage was 30 J.

## 2.2. Experiment procedures

The calcified montmorillonite powder sample used in this study was produced by Shanghai Aladdin Biochemical Technology Co., Ltd. Calcified montmorillonite powder with a mass of 15 g and particle sizes of 21–32  $\mu\text{m}$ , 41–52  $\mu\text{m}$ , 61–72  $\mu\text{m}$ , and 81–92  $\mu\text{m}$  was selected for the explosion suppression experiments. The powder driven by carbon dioxide gas with a volume fraction of 20% to lift and suspend the powder in the pipeline, and the gas injection pressure was set to 0.15 MPa (Wang et al., 2021; Wang et al., 2019). The ambient temperature and pressure during the experiment are 24–26  $^{\circ}\text{C}$  and 0.1 MPa, respectively.

The experimental gas is distributed according to Dalton's law of partial pressure. A vacuum pump is used to inject the prepared methane-air gas into the explosion chamber. Use a circulation pump to circulate the gas for 20 min, ensuring that the methane and air mix well. At the end of each experiment, the Air compressor was used for 30 min for ventilation to vent the residual gas from the explosion. Before the experiment started, the explosion chamber was filled with a preconfigured methane test gas with a volume fraction of 9.5% and an equiv-

alence ratio of 1. The polytetrafluoroethylene film was used to separate the explosion chamber from the pipe network. The pressure sensors were installed at the eight monitoring points shown in Fig. 1, and two flame photosensitive sensors were installed at the two outlets to detect the time when the explosion flame wave reached the outlets. The calcified montmorillonite powder was laid in the pipeline and the laying position is shown in Fig. 1. The air jet device was started, and the jet was started and continued for 15 s. Subsequently, ignition was performed and the switch for the external trigger device was turned on. At the same time, the igniter and the data acquisition system started working synchronously.

Each group of experiments was repeated three times, and the experimental data were taken as the arithmetic mean of the three experiments. After the experiment, the exhaust gas in the pipeline was discharged and gas cleaning was carried out in the pipeline.

## 2.3. Powder material characteristics

The calcified montmorillonite powders with different particle size ranges were screened out using sieves of different sizes. The particle size distribution test of the powders in the selected four particle size ranges was carried out using a model Winner 2018 laser particle size analyzer test results are shown in Fig. 2.

It can be seen from Fig. 2 that the particle size distribution of the powder used in the experiment relatively uniform, and the powder sample experimental requirements.

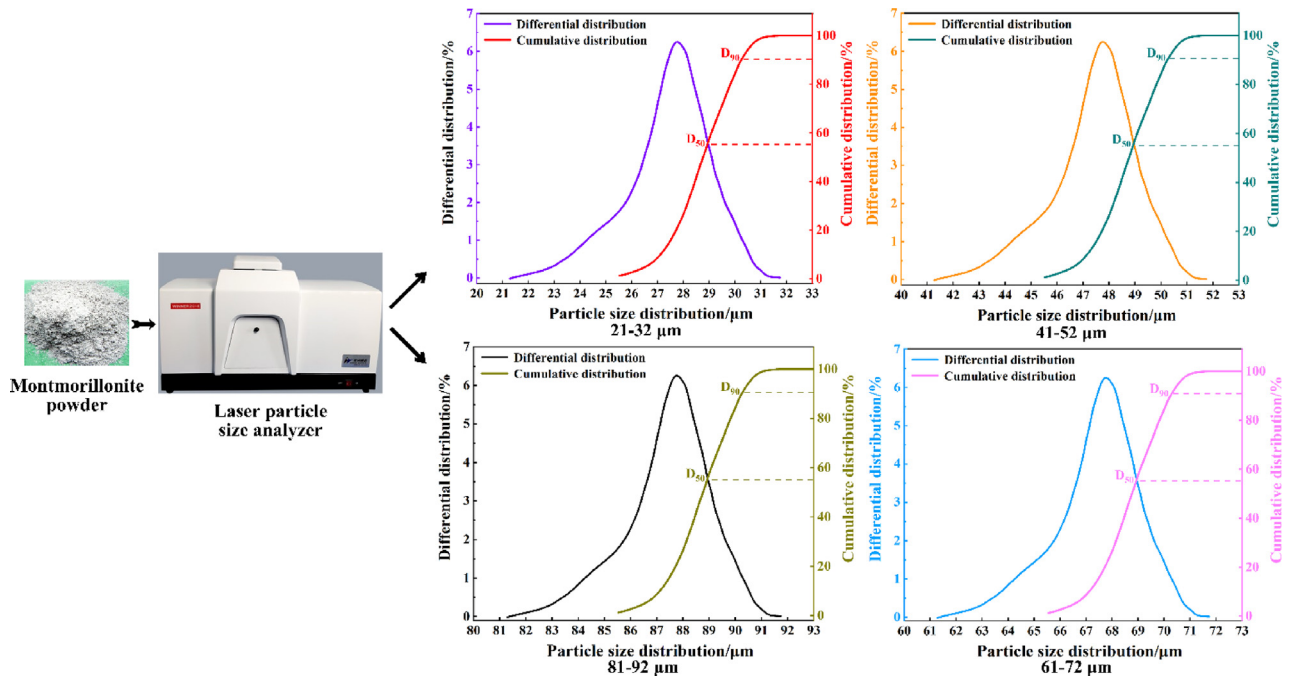


Fig. 2 Particle size distribution of the calcified montmorillonite powder sample.

Due to its unique layered molecular structure, the calcified montmorillonite powder contains a large number of water molecules and structural hydrate crystals between the molecular layers, in addition to the surface adsorption of water. Component analysis of the sample powder was carried out using a Shimadzu 6100 X-ray diffractometer, and the results are shown in Fig. 3. The strong diffraction peak at the  $2\theta$  angle of  $7.26^\circ$  to the 001-crystal plane of montmorillonite. The calculated crystal plane spacing was 1.54 nm, which the powder sample used in the experiment calcified montmorillonite. The diffraction peaks at  $2\theta$  angles of  $19.78^\circ$ ,  $21.96^\circ$ , and  $35.91^\circ$  correspond to the 100, 101, and 114 crystal planes of the calcified montmorillonite powder, respectively (Wang et al., 2019).

### 3. Results and analysis

#### 3.1. Suppression effect of the powder particle size on the explosion overpressure

The overpressure evolution process of monitoring point 1 under different working conditions is shown in Fig. 4. Under the condition of no explosion suppression, the explosion overpressure fluctuated many times indicating that the explosion shock wave experienced multiple superposition and hedging throughout the propagation process. Because the shock wave was affected by the pipe network structure during the propagation process and presented a complex and disordered state, the explosion overpressure presented multi-peak characteristics, and the maximum overpressure in the whole process was 0.4611 MPa. Under each explosion suppression condition, the complex disorder of the shock wave during the propagation process gradually weakened and eventually disappeared, resulting in single peak characteristic of the explosion overpressure. The principal reason was mainly suppression of the chemical reaction rate of the methane explosion during the ini-

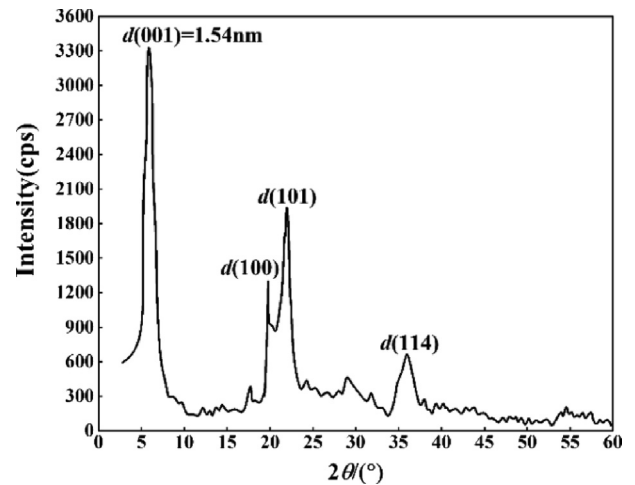


Fig. 3 XRD pattern of the calcified montmorillonite powder.

tial stage of the explosion, and some intermediate steps in the chain reaction that characterized the chemical reaction process could not be carried out normally, as well as the active attenuation characteristics of the shock wave during the propagation process (Niu et al., 2019; Niu et al., 2021). As a result, the multiple superposition and attenuation processes of the shock wave almost disappeared, and the peak overpressure dropped significantly.

When the particle size of the calcified montmorillonite powder was 21–32  $\mu\text{m}$ , the explosion overpressure dropped sharply during the later stage of the reaction. The particle size of the powder was too small, and the inhibitory effect on the explosion overpressure during the early stage of the reaction was better than the other particle sizes. However, in the middle

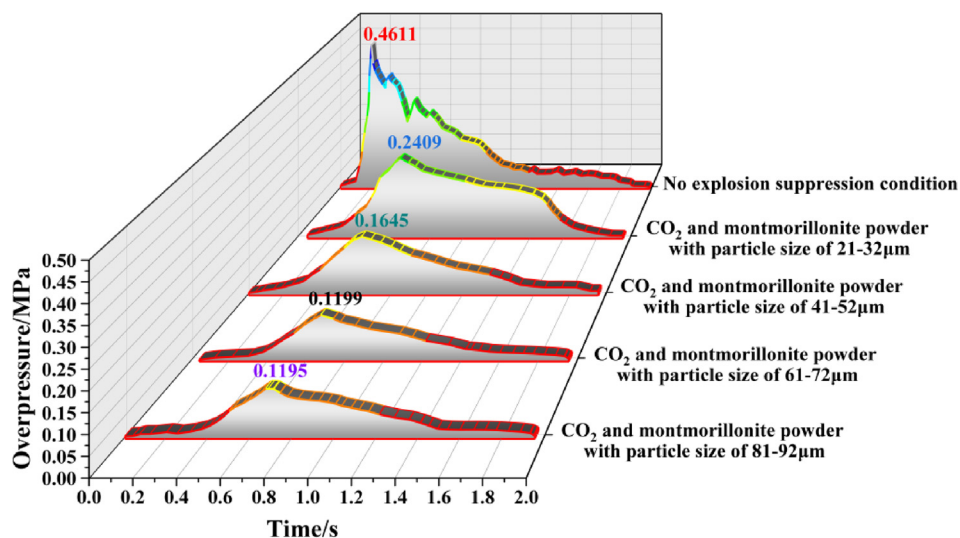


Fig. 4 Evolution process of explosion overpressure at monitoring point 1 under different working conditions.

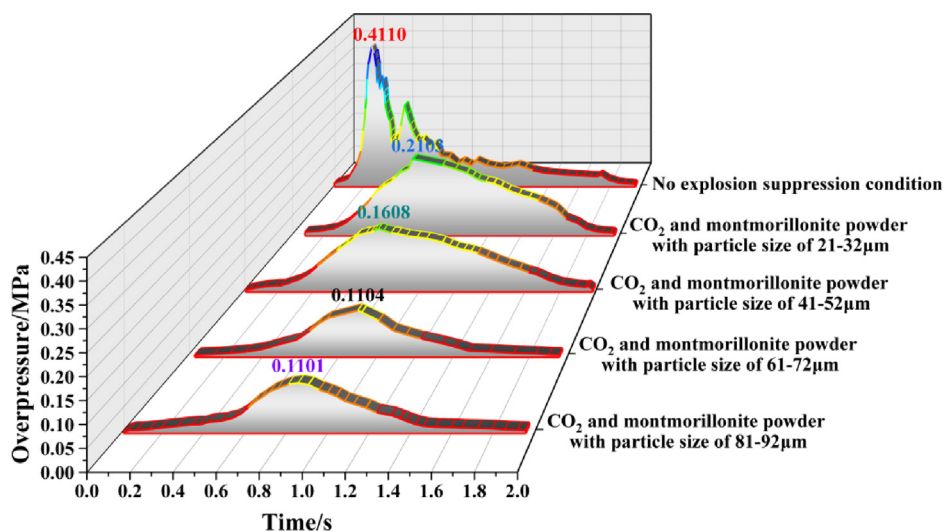


Fig. 5 Evolution process of explosion overpressure at monitoring point 2 under different working conditions.

and later stages of the reaction, the strength of the shock wave decreased significantly with continuous attenuation resulting in a sharp drop in explosion overpressure. The maximum overpressure during the entire process dropped by about 50% to 0.2409 MPa, and the time to reach the peak of overpressure increased significantly. As the particle size of the powder increased, the explosion overpressure showed a steady downward trend, and the peak overpressure decreased further to 0.1645 MPa, 0.1199 MPa, and 0.1195 MPa, and the time to reach the peak of overpressure was continuously delayed. When the particle size of the powder increased from 61 to 72 to 81–92  $\mu\text{m}$ , the overpressure peak only decreased slightly indicating that the powder particle size of 61–72  $\mu\text{m}$  had a better inhibitory effect on the overpressure of methane explosion.

Figs. 5 to 11 show the overpressure evolution process from monitoring points 2 and 8 under different working conditions. In general, the overpressure evolution process of the other

monitoring points was similar to monitoring point 1. Overpressure peaks at all the other monitoring points under different working conditions, the particle size of the calcified montmorillonite powder increased from 61 to 72 to 81–92  $\mu\text{m}$ , in the range of peak overpressure was very small, and the time to reach the was almost the same. Therefore, reducing the overpressure peak value, the calcified montmorillonite powder, and using a particle size of 6172  $\mu\text{m}$  had the best suppression effect on the explosion overpressure.

The overpressure evolution process of all the monitoring points could be summarized by the following points. The effect of the pipe network structure on the propagation characteristics of the explosion shock wave was greatly weakened and presented similar propagation characteristics as those in long straight pipes (Zhou et al., 2019), indicating that the carbon dioxide-driven calcified montmorillonite powder can effectively suppress the methane explosion in the pipe network

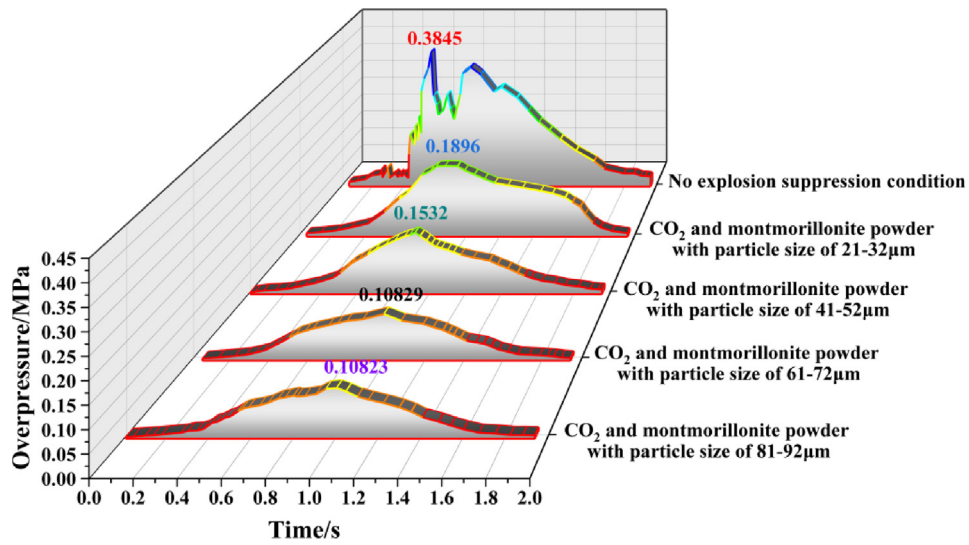


Fig. 6 Evolution process of explosion overpressure at monitoring point 3 under different working conditions.

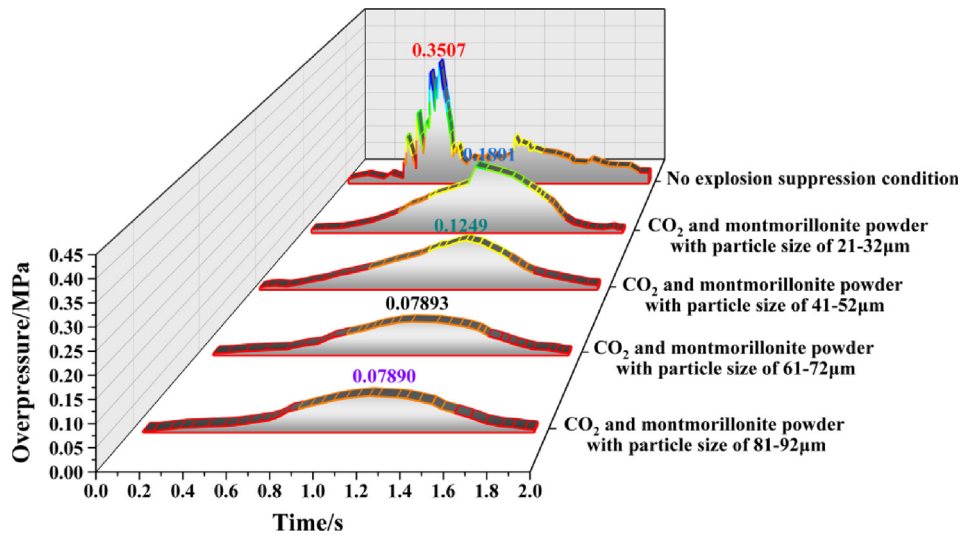


Fig. 7 Evolution process of explosion overpressure at monitoring point 4 under different working conditions.

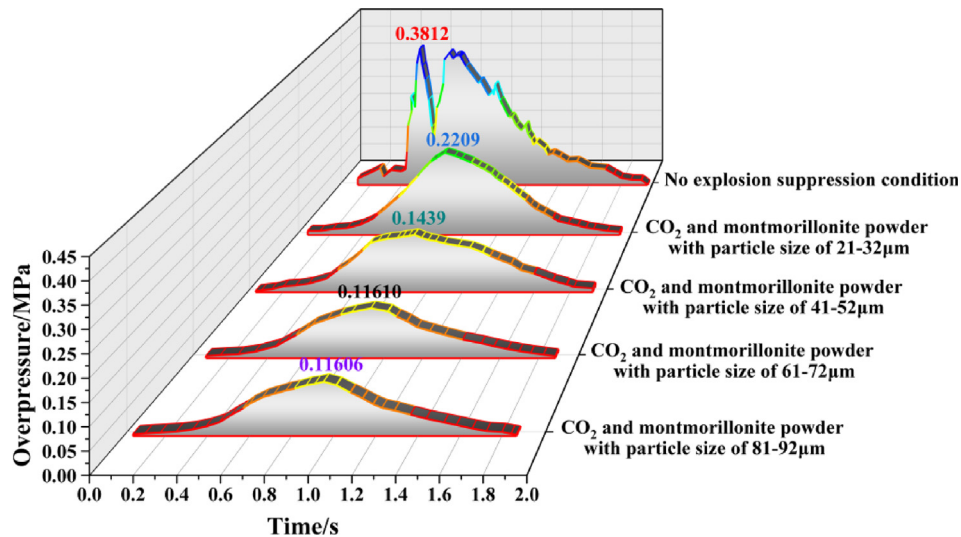


Fig. 8 Evolution process of explosion overpressure at monitoring point 5 under different working conditions.

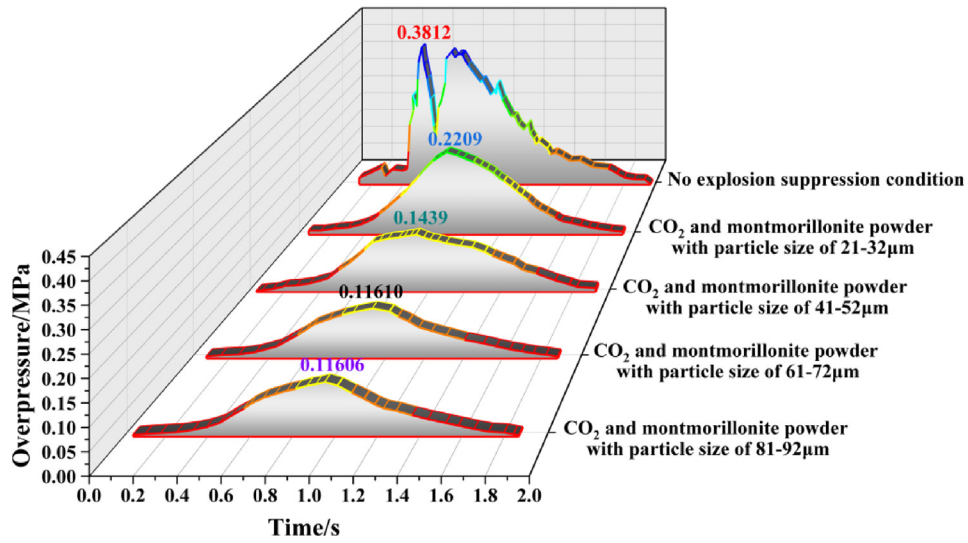


Fig. 9 Evolution process of explosion overpressure at monitoring point 6 under different working conditions.

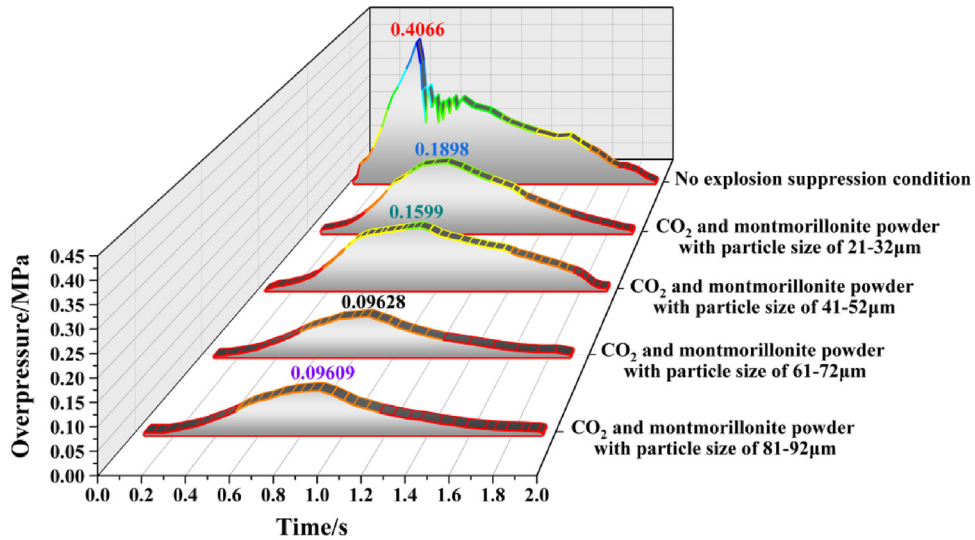


Fig. 10 Evolution process of explosion overpressure at monitoring point 7 under different working conditions.

(Sun et al., 2020). The effectiveness of this explosion suppression method serves as a basis for methane explosion suppression in actual pipe networks.

### 3.2. Effect of powder particle size on explosion power index

The explosive power index is a vital parameter of the destructive power of methane explosions. The explosive power index (Yang et al., 2018) is defined by:

$$K = P_{\max} v \quad (1)$$

where  $K$  is the power index ( $10^{12} \text{ Pa}^2/\text{s}$ ),  $P_{\max}$  is the peak value of the explosion overpressure (MPa), and  $v$  is the average rate of increase in the explosion overpressure (MPa/s).

The average rate of increase in the explosion overpressure is defined as:

$$v = \frac{P_{\max} - P_0}{\Delta t} \quad (2)$$

where  $P_{\max}$  is the peak value of explosion overpressure (MPa),  $P_0$  is the initial explosion overpressure (MPa) and  $\Delta t$  is the time required to go from the initial explosion overpressure to the peak explosion overpressure (s).

The peak values of the explosion overpressure and the average increase rates of the explosion overpressure at all monitoring points under the working conditions of the calcified montmorillonite powder with different particle sizes are shown in Table 1. Based on the data in Table 1, the explosion power index values of all monitoring points under the suppression conditions of the different calcified montmorillonite powder particle sizes were calculated (shown in Fig. 12).

Fig. 12 shows the variation law of the explosion power index within calcified montmorillonite powder particle size lin-

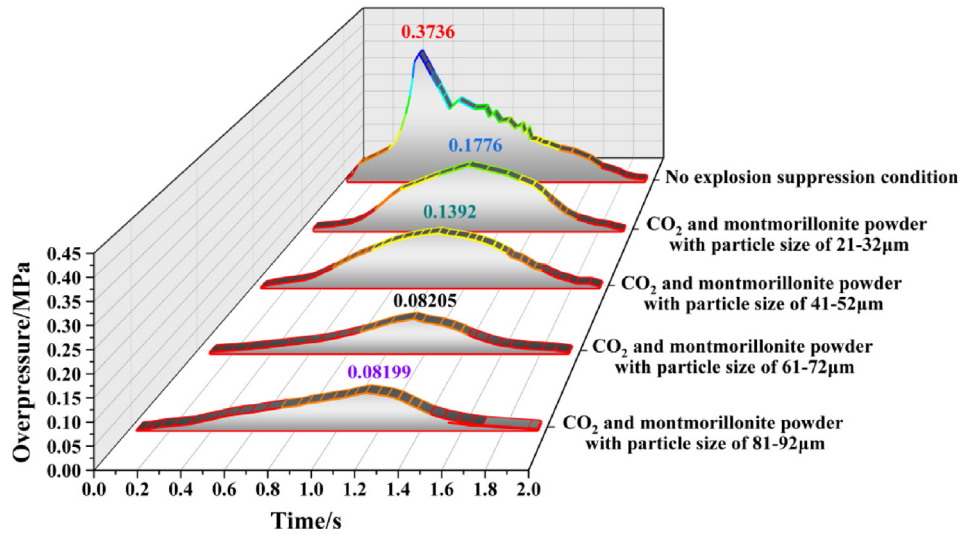


Fig. 11 Evolution process of explosion overpressure at monitoring point 8 under different working conditions.

early related to the variation law of the explosion overpressure with increasing calcified montmorillonite powder particle size. Thus, the explosion power index of each monitoring point showed a decreasing trend in powder particle size. When the particle size of the calcified montmorillonite powder increased from 61 to 72 to 81–92  $\mu\text{m}$ , the explosion power index of monitoring point 1 and monitoring point 8 remained unchanged, and the explosion power index values of the other monitoring points decreased slightly. We found that within a certain particle size range, the explosion power index decreased in particle size of the calcified montmorillonite powder. After exceeding the critical value of the particle size, the explosion power index remained almost unchanged. When the particle size of the calcified montmorillonite powder was 61–72  $\mu\text{m}$ , the suppression effect on the explosion power index was the most effective.

### 3.3. Suppression effect of the powder particle size on explosion flame propagation

Fig. 13 shows the time required for the explosion flame wave to reach the outlets of the two pipe networks; the time to reach outlet 1 was greater than the time to reach outlet 2. Within the particle size of the calcified montmorillonite powder, the propagation of the explosion flame wave was further effectively suppressed. The change in powder particle size showed a significant impact on the suppression effect of the explosion flame wave. When the particle size of the calcified montmorillonite powder was 61–72  $\mu\text{m}$ , the normal propagation of the flame wave was effectively suppressed, and particle size of the powder continued to increase to 81–92  $\mu\text{m}$ . The time for the flame wave to reach outlet 1 did not increase, while the time for the flame wave to reach outlet 2 increased by only 1 ms.

Previous studies have demonstrated that the smaller the particle size of the powder explosion inhibitor, the more conducive it will be to explosion suppression. Because the powder with a smaller particle size had a smaller specific surface area when participating in the reaction and a larger effective contact area with the shock wave and flame wave generated by the explosion, it was able to more fully participate in the explo-

sion suppression reaction (Zhou et al., 2019; Sun et al., 2020; Jiang et al., 2019; Zheng et al., 2014). Therefore, from the perspective of the suppression effect on flame propagation, the explosion suppression effect of the calcified montmorillonite powder was the best when the particle size was 61–72  $\mu\text{m}$ .

### 3.4. Discussion

In summary, when comparing the suppression performance of the different calcified montmorillonite powder particle sizes on the explosion overpressure, explosion power index, and explosion flame propagation, and considering the practical significance of providing a reference for actual working conditions, the calcified montmorillonite powder with the best explosion suppression performance was obtained with a particle size of 61–72  $\mu\text{m}$ .

Under the condition of no explosion suppression, the propagation process of the shock waves and flame waves of methane explosion is nonlinear and disordered. The changes in the explosion overpressure peak and the explosion power index do not show a regular linear decrease with increasing distance from the explosion source. In addition, in terms of the time taken for the flame wave to propagate to the two pipe network outlets, the pipe network structure makes the effectiveness of the explosion suppressor more prominent. With an increasing powder particle size (within a certain range), the time increment gradient for the flame wave to propagate to the outlet farther away from the explosion source is larger. These characteristics are not found in spherical containers or horizontal straight pipes. Under explosion suppression conditions (especially the optimal explosion suppression condition), the influence of the pipe network structure on methane explosion is greatly attenuated, and the explosion overpressure peak and explosion power index at different monitoring points in the pipe network show a linear variation similar to that in a straight horizontal pipe. However, the difference is that the characteristics similar to linear but not completely the same as the horizontal straight pipe in the pipe network can just explain the necessity for studying explosion suppression in the pipe network. More importantly, the conclusion of the

**Table 1** The peak explosion overpressure and average explosion overpressure rise rate data for different powder sizes.

Particle size of the powder	M <sub>1</sub>		M <sub>2</sub>		M <sub>3</sub>		M <sub>4</sub>		M <sub>5</sub>		M <sub>6</sub>		M <sub>7</sub>		M <sub>8</sub>	
	$P_{\max}$	$\gamma$														
0	0.4611	2.189	0.4110	1.625	0.3845	0.663	0.3507	0.569	0.3812	0.54	0.4133	0.819	0.4066	0.935	0.3736	0.754
21–32 $\mu\text{m}$	0.2409	0.3837	0.2103	0.281	0.1896	0.216	0.1801	0.207	0.2209	0.249	0.2103	0.266	0.1898	0.224	0.1776	0.175
41–52 $\mu\text{m}$	0.1645	0.2563	0.1608	0.208	0.1532	0.165	0.1249	0.171	0.1439	0.155	0.1489	0.168	0.1599	0.176	0.1392	0.133
61–72 $\mu\text{m}$	0.1199	0.1719	0.1104	0.1225	0.10829	0.1087	0.07893	0.072	0.11610	0.123	0.09956	0.09	0.09628	0.112	0.08205	0.073
81–92 $\mu\text{m}$	0.1195	0.1719	0.1101	0.1224	0.10823	0.1082	0.07890	0.070	0.11606	0.122	0.09915	0.091	0.09609	0.109	0.08199	0.073

effectiveness of the explosion suppressor and the optimal explosion suppression parameters in the pipe network is more general and universal.

#### 4. Analysis of explosion suppression mechanism

The pyrolytic properties of the calcified montmorillonite powder showed that it had good physical explosion suppression properties, and the chemical composition of the calcified montmorillonite powder showed that it effectively inhibits the chain reactions of methane explosions (Uddin, 2008; Babushok et al., 2017). In addition, as an effective methane explosion inhibitor, carbon dioxide not only had the same physical explosion suppression mechanism as the inert gas, but it also participated in the branch reaction of the methane explosion (Chuanbo et al., 2018). Therefore, the suppression of carbon dioxide-driven calcified montmorillonite powder on methane explosions was considered a composite effect of physical and chemical suppression.

With respect to physical suppression processes, the thermogravimetry-differential scanning calorimetry-derivative thermogravimetry (TG-DSC-DTG) curves of the calcified montmorillonite powders are shown in Fig. 14. The thermal decomposition of the calcified montmorillonite powder can be divided into 3 stages, namely, 0–240 °C, 240–725 °C, and 725–770 °C. The first stage is a desorption process of physically adsorbed water on the surface of the montmorillonite, while the second stage includes the desorption of the adsorbed water between the montmorillonite crystal layers, and the third stage is the destruction of the montmorillonite lattice (Guo et al., 2005). Two hydroxyl groups were released in the form of one water molecule, and the structural water was lost. The DTG curve shows a strong heat absorption peak in the first stage where the temperature peak was 69 °C. The thermal decomposition rate was 0.1395 mg/min. In addition, the total energy absorbed by the calcified montmorillonite powder throughout the pyrolysis process was calculated to be 390.72 J/g. These parameters fully demonstrate the excellent endothermic properties of the calcified montmorillonite powder (Wang et al., 2016).

During the explosion process, the water vapor generated by the thermal decomposition of the calcified montmorillonite powder not only dilutes the oxygen concentration in the reaction system but also absorbs a large amount of heat generated during the explosion process. The heat loss in the entire reaction system is greater than the heat release, and the heat transfer in methane inhibited to a certain extent, the physical suppression of the methane explosion (Krasnyansky, 2006). In addition, as an inert substance diluting the fuel-air mixture, carbon dioxide effectively reduces the concentration of combustible gas reactants in the reaction system, hindering the transfer of heat to the combustible gas. Specifically, it reduces the possibility of contact between the combustible gas and oxygen molecules and the effective contact surface area, achieving the purpose of physical explosion suppression (Pei et al., 2016; Chen et al., 2015).

As for chemical suppression, the radicals  $\cdot\text{O}$ ,  $\text{H}\cdot$ , and  $\cdot\text{OH}$  were shown to play a key role in methane explosion chain reactions. The metal ions generated during the thermal dehydration of calcified montmorillonite powder will combine with the key active radicals  $\cdot\text{O}$ ,  $\text{H}\cdot$  and  $\cdot\text{OH}$  generated by

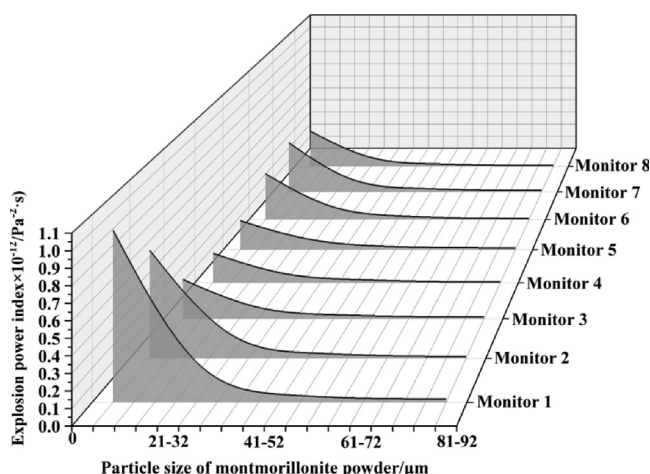


Fig. 12 Explosive power index values for all monitoring points under different powder particle size conditions.

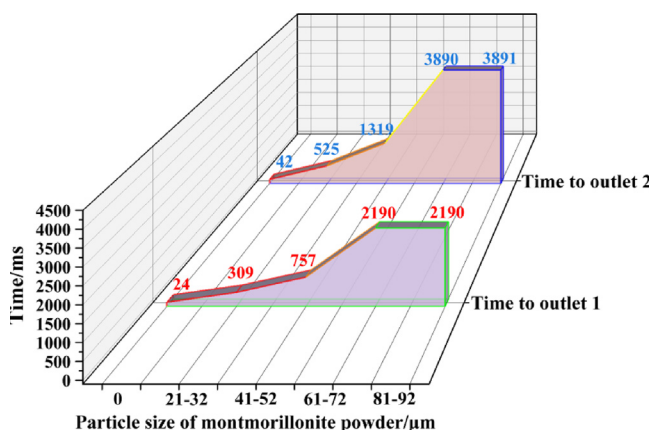


Fig. 13 Times for the explosion flame wave to reach the two outlets under different conditions.

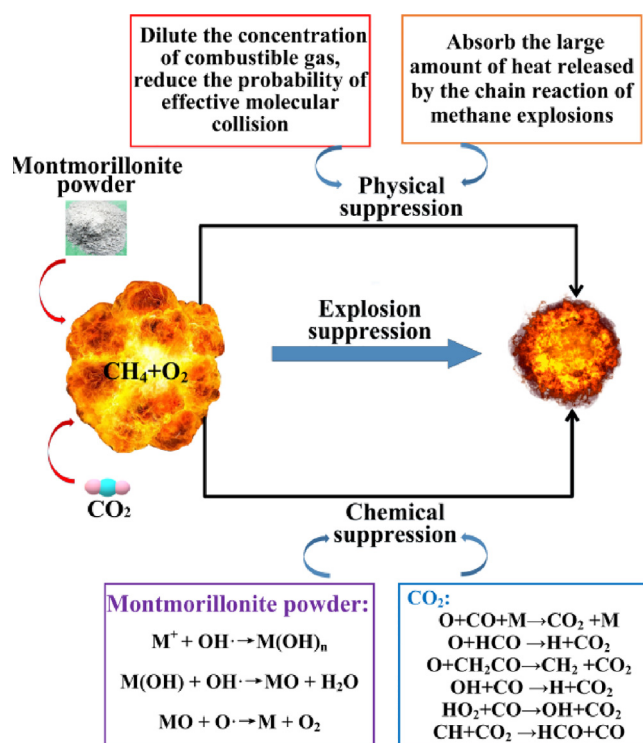


Fig. 15 Schematic diagram showing the explosion suppression mechanism.

the methane explosion to produce chemical reactions (Krasnyansky, 2008; Ni et al., 2011). The key steps that will affect the chain reaction rate are:

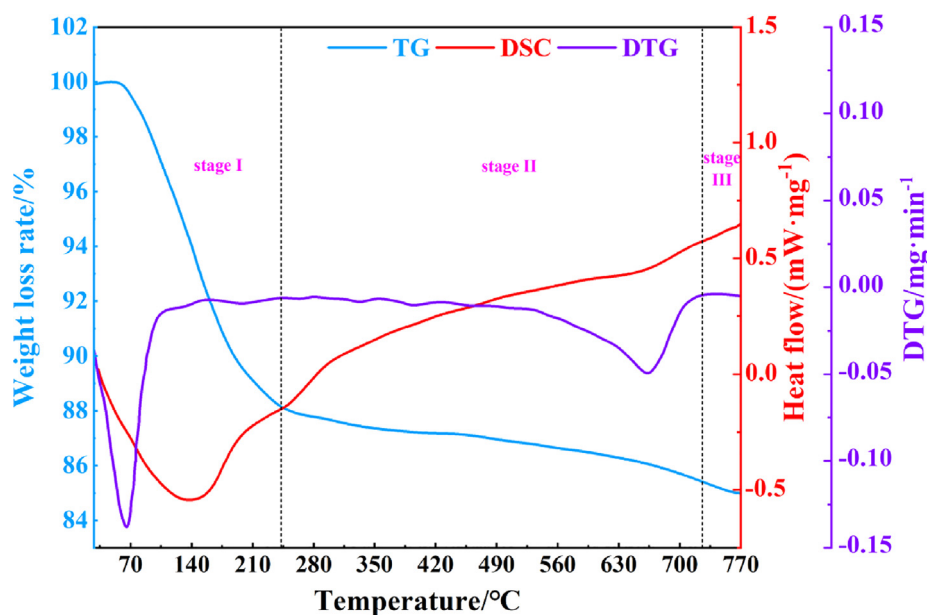
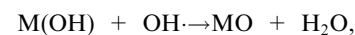
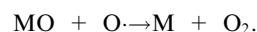
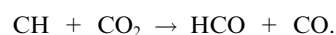
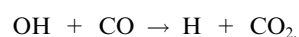
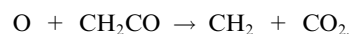
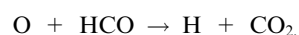


Fig. 14 TG-DSC-DTG curves of the calcified montmorillonite powder.



Because  $\text{CO}_2$  itself was one of the products in the methane explosion reaction, the addition of carbon dioxide affected the direction of the reaction as carbon dioxide was converted into CO through the reaction. Additionally, the CO reduced the concentration of important free radicals that maintained the methane explosion reaction and burning rates (Li et al., 2019; Chen et al., 2021). The reaction chain transfer processes after adding carbon dioxide are as follows:



The above reactions effectively consume the intermediate free radicals in the methane explosion chain reaction products and the chain reaction carrier by inhibiting regeneration, greatly reducing the number of active free radicals in the entire reaction system, interrupting the chain reaction of the explosion reaction, and realizing the purpose of chemical explosion suppression (Nie et al., 2017).

In summary, a mechanism diagram for methane explosion by carbon dioxide-calcified montmorillonite powder was obtained, as shown in Fig. 15.

## 5. Conclusions

In this work, we studied the suppression effect of carbon dioxide-driven calcified montmorillonite powders with different particle sizes on methane explosion in an experimental pipe network, and we analyzed the explosion suppression mechanism. The conclusions are summarized as follows:

- (1) Carbon dioxide-driven calcified montmorillonite powder can effectively suppress the propagation of shock waves and flame waves that are generated by methane explosions in pipe networks from the perspective of the explosion overpressure peaks, the explosion power indexes and the times taken for the flame wave to reach the two outlets of the pipe network. Overall, the calcified montmorillonite powder with a particle size of 61–72  $\mu\text{m}$ , and the calcified montmorillonite powder with a particle size of 81–92  $\mu\text{m}$ , had almost the same inhibition performance on methane explosion. Considering the cost of use in practical applications, the calcified montmorillonite powder with a particle size of 61–72  $\mu\text{m}$  is the optimal detonation inhibitor.
- (2) Carbon dioxide and calcified montmorillonite powder suppress methane explosion mainly through physical suppression and chemical suppression. With respect to physical suppression processes, calcified montmorillonite powder can not only effectively mitigate the oxygen concentration in the reaction system, but also absorb a large amount of energy and heat generated in the explosion process. In addition, carbon dioxide can effectively mitigate the concentration of combustible gas reactants in the reaction system, and hinder the transfer of heat

to the combustible gas. As for chemical suppression, the metal ions generated by the calcified montmorillonite powder in the process of thermal dehydration can chemically react with the key active groups generated by methane explosion, effectively reducing the activation energy in the entire reaction. Carbon dioxide can not only suspend the positive reaction rate of methane and oxygen, but also react with oxygen in the reaction system, effectively reducing the concentration of important free radicals that maintain the methane explosion reaction.

- (3) On the basis of the calcified montmorillonite, compound explosion suppression with carbon dioxide can serve as a theoretical reference and support for further improving the safety of methane extraction, transportation, and utilization.

In the future work, we will study the influence of the mineral and chemical composition of calcified montmorillonite on the suppression of methane explosion. At the same time, in order to make the whole research process more visible, it is planned to build a transparent experimental pipe network to study the synergistic explosion suppression performance of different volume fractions of carbon dioxide and calcified montmorillonite powder with different particle sizes and masses.

## Declaration of Competing Interest

The authors declare that they have no known competing financial interests or personal relationships that could have appeared to influence the work reported in this paper.

## Acknowledgements

This work was partly supported by the National Natural Science Foundation of China (grant number 52174183), and the Natural Science Foundation of Liaoning Province (grant number 2019-MS-162).

## Author contributions

Wang Fengxiao: Performed the experiment, manuscript preparation and writing original manuscript. Jia Jinzhang.: Formal analysis and contributed to the conception of the study. Tian Xiuyuan: Contributed significantly to the data analysis.

## References

- Babushok, V., Linteris, G., Hoorelbeke, P., et al, 2017. Flame inhibition by potassium-containing compounds. *Combust. Sci. Technol.* 189, 2039–2055.
- Cao, X., Ren, J., Bi, M., et al, 2016. Experimental research on methane/air explosion inhibition using ultrafine water mist containing additive. *J. Loss Prev. Process Ind.* 43, 352–360.
- Chen, X., Ding, Y., Cheng, F., et al, 2015. Influence of  $\text{CO}_2$  on explosion suppression characteristics of multicomponent flammable gas in coal mine. *Coal Sci. Technol.* 43 (03), 43–47.
- Chen, F., Nan, F., Luo, Z., et al, 2021. Research progress and development trend of gas explosion suppression materials and mechanism. *Coal Sci. Technol.* 49 (08), 114–124.
- Cheng, J., Wang, C., Zhang, S., 2012. Methods to determine the mine gas explosibility—an overview. *J. Loss Prev. Process Ind.* 25 (03), 425–435.
- Chuanbo, C., Hao, S., Shuguang, J., et al, 2018. Experimental study on gas explosion suppression by coupling  $\text{CO}_2$  to a vacuum chamber. *Powder Technol.* 335, 42–53.

- Cui, C., Shao, H., Jiang, S., et al. 2018. Experimental study on gas explosion suppression by coupling CO<sub>2</sub> to a vacuum chamber. *Powder Technol.* 335, 42–53.
- Dong, C., Bi, M., Zhou, Y., 2012. Effects of obstacles and deposited coal dust on characteristics of premixed methane–air explosions in a long-closed pipe. *Saf. Sci.* 50, 1786–1791.
- Guo, Q., Ren, W., Zhu, J., et al. 2019. Study on the composition and structure of foamed gel for fire prevention and extinguishing in coal mines. *Process Saf. Environ. Prot.* 128, 176–183.
- Guo, Z., Xing, R., Liu, S., et al. 2005. The synthesis and antioxidant activity of the Schiff bases of chitosan and carboxymethyl chitosan. *Bioorg. Med. Chem. Lett.* 15 (20), 4600–4603.
- Jia, J., Wang, F., Li, J., et al. 2022. Propagation characteristics of the overpressure waves and flame fronts of methane explosions in complex pipeline networks. *Geomatics, Nat. Hazards Risk* 13 (01), 54–74.
- Jiang, H., Bi, M., Li, B., et al. 2019. Flame inhibition of aluminum dust explosion by NaHCO<sub>3</sub> and NH<sub>4</sub>H<sub>2</sub>PO<sub>4</sub>. *Combust. Flame* 200, 97–114.
- Jiang, H., Bi, M., Peng, Q., Gao, W., 2020. Suppression of pulverized biomass dust explosion by NaHCO<sub>3</sub> and NH<sub>4</sub>H<sub>2</sub>PO<sub>4</sub>. *Renew Energy* 147 (2020), 2046–2055.
- Jiang, B., Liu, Z., Tang, M., et al. 2016. Active suppression of premixed methane/air explosion propagation by non-premixed suppressant with nitrogen and ABC powder in a semi-confined duct. *J. Nat. Gas Sci. Eng.* 29, 141–149.
- Jing, Q., Wang, D., Liu, Q., et al. 2021. Inhibition effect and mechanism of ultra-fine water mist on CH<sub>4</sub>/air detonation: quantitative research based on CFD technology. *Process Saf. Environ. Prot.* 148, 75–92.
- Krasnyansky, M., 2006. Prevention and suppression of explosions in gas-air and dust-air mixtures using powder aerosol-inhibitor. *J. Loss Prev. Process Ind.* 19 (06), 729–735.
- Krasnyansky, M., 2008. Studies of fundamental physical chemical mechanisms and processes of flame extinguishing by powder aerosols. *Fire Mater.* 32 (01), 27–47.
- Kundu, S., Zanganeh, J., Moghtaderi, B., 2016. A review on understanding explosions from methane-air mixture. *J. Loss Prev. Process Ind.* 40, 507–523.
- Li, H., Deng, J., Chen, X., et al. 2020. Qualitative and quantitative characterization for explosion severity and gaseous-solid residues during methane-coal particle hybrid explosions: an approach to estimating the safety degree for underground coal mines. *Process Saf. Environ. Prot.* 141, 150–166.
- Li M, Xu J, Wang C, et al. Thermal and kinetics mechanism of explosion mitigation of methane-air mixture by N<sub>2</sub>/CO<sub>2</sub> in a closed compartment. *Fuel*, 255(2019):115747.
- Luo Z, Su Y, Chen X, et al. Effect of BC powder on hydrogen/methane/air premixed gas deflagration. *Fuel*, 257(2019):116095.
- Ni, X., Chow, W., Li, Q., et al. 2011. Experimental study of new gas-solid composite particles in extinguishing cooking oil fires. *J. Fire Sci.* 29 (02), 152–176.
- Nie, B., Yang, L., Ge, B., et al. 2017. Chemical kinetic characteristics of methane/air mixture explosion and its affecting factors. *J. Loss Prev. Process Ind.* 49, 675–682.
- Niu, Y., Shi, B., Jiang, B., 2019. Experimental study of overpressure evolution laws and flame propagation characteristics after methane explosion in transversal pipe networks. *Appl. Therm. Eng.* 154, 18–23.
- Niu, Y., Zhang, L., Shi, B., et al. 2021. Methane-coal dust mixed explosion in transversal pipe networks. *Combust. Sci. Technol.* 193 (10), 1734–1746.
- Pei, B., Yu, M., Chen, L., et al. 2016. Experimental study on the synergistic inhibition effect of gas-liquid two phase medium on gas explosion. *J. Loss Prev. Process Ind.* 49 (01), 797–804.
- Song, Y., Zhang, Q., 2018. The quantitative studies on gas explosion suppression by an inert rock dust deposit. *J. Hazard. Mater.* 353, 62–69.
- Sun, Y., Yuan, B., Chen, X., et al. 2019. Suppression of methane/air explosion by kaolinite-based multi-component inhibitor. *Powder Technol.* 343, 279–286.
- Sun, Y., Yuan, B., Shang, S., et al. 2020. Surface modification of ammonium polyphosphate by supramolecular assembly for enhancing fire safety properties of polypropylene. *Compos. Part B-Eng.* 181, (2020) 107588.
- Uddin, F., 2008. Clays, nanoclays, and montmorillonite minerals. *Metall. Mater. Trans. A* 39 (12), 2804–2814.
- Wang Y, Meng X, Ji W, et al. 2019. The inhibition effect of gas-solid two-phase inhibitors on methane explosion. *Energies*, 2019,12 (03):398.
- Wang T, Luo Z, Wen H, et al. The explosion enhancement of methane-air mixtures by ethylene in a confined chamber. *Energy*, 214(2021):119042.
- Wang Y, Lin S, Feng H, et al. Suppression of different functional group modified powders on 9.5% CH<sub>4</sub>-air explosion and molecular simulation mechanism. *Journal of Loss Prevention in the Process Industries*, 69(2021): 104344.
- Wang, Y., Feng, H., Zhang, Y., et al. 2019. The inhibition effect of gas–solid two-phase inhibitors on methane explosion. *Energies* 12 (21), 1–12.
- Wang, J., Hu, S., Nie, S., et al. 2016. Reviews on mechanisms of in vitro antioxidant activity of polysaccharides. *Oxid. Med. Cell. Longevity* 2016, 5692852.
- Wang, L., Liang, Y., Hu, Y., Hu, W., 2020. Synergistic suppression effects of flame retardant, porous minerals and nitrogen on premixed methane/air explosion. *J. Loss Prev. Process Ind.* 67.
- Wang, Y., Ying, H., Meng, H., et al. 2019. Investigation of the effect of montmorillonite powders on gas explosion parameters. *Trans. Beijing Inst. Technol.* 39 (02), 111–117.
- Wang, Y., Lin, S., Li, Z., et al. 2021. Research on synergistic effect of inert gas on methane explosion suppression performance of KHCO<sub>3</sub> cold aerosol. *Coal Sci. Technol.* 49 (02), 145–152.
- Wang, Y., Lin, S., Li, Z., et al. 2021. Influence of dispersion pressure on methane explosion suppression effect of KHCO<sub>3</sub> cold aerosol. *China Saf. Sci. J.* 31 (7), 70–75.
- Wen, X., Wang, M., Su, T., et al. 2019. Suppression effects of ultrafine water mist on hydrogen/methane mixture explosion in an obstructed chamber. *Int. J. Hydrogen Energy* 44 (60), 32332–32342.
- Yang K, Chen K, Ji H, et al. Experimental study on the effect of modified attapulgite powder with different outlet blockage ratios on methane-air explosion. *Energy*, 237(2021):121675.
- Yang, K., Ji, H., Xing, Z., et al. 2018. Characteristics on methane explosion suppression by ultrafine water mist containing potassium oxalate. *CIESC J.* 69 (12), 5359–5369.
- Yang, H., Lin, Y., Liu, C., et al. 2019. Suppression of flame propagation in a long duct by inertia isolation with inert gases. *J. Loss Prev. Process Ind.* 59, 23–34.
- Yu, M., Wang, X., Zheng, K., et al. 2020. Investigation of methane/air explosion suppression by modified montmorillonite inhibitor. *Process Saf. Environ. Prot.* 144, 337–348.
- Yu, M., Liu, M., Wen, X., et al. 2022. Experimental study on suppression of methane explosion by porous media and ultra-fine water mist. *Energy Sources Part A* 44 (01), 1751–1764.
- Zhang, B., Chang, X., Bai, C., 2020. End-wall ignition of methane-air mixtures under the effects of CO<sub>2</sub>/Ar/N<sub>2</sub> fluidic jets. *Fuel* 270, (2020) 117485.
- Zheng, L., Zheng, K., Pan, R., et al. 2014. Inhibition of the premixed CH<sub>4</sub>/air deflagration by powdered extinguishing agents. *Procedia Eng.* 71, 230–237.
- Zhou, J., Li, B., Ma, D., et al. 2019. Suppression of nano-polymethyl methacrylate dust explosions by ABC powder. *Process Saf. Environ. Prot.* 122, 144–152.
- Zhou, Y., Li, Y., Jiang, H., et al. 2021. Investigations on unconfined large-scale methane explosion with the effects of scale and obstacles. *Process Saf. Environ. Prot.* 155, 1–10.